Cusp singularities in the distribution of orientations of asymmetrically pivoted hard disks on a lattice

Sushant Saryal [1,2,*] and Deepak Dhar [1,†]

[1]*Department of Physics, Indian Institute of Science Education and Research, Pune 411008, India*
[2]*Department of Chemistry, Princeton University, Princeton, New Jersey 08544, USA*

We study a system of equal-size circular disks, each with an asymmetrically placed pivot at a fixed distance from the center. The pivots are fixed at the vertices of a regular triangular lattice. The disks can rotate freely about the pivots, with the constraint that no disks can overlap with each other. Our Monte Carlo simulations show that the one-point probability distribution of orientations has multiple cusplike singularities. We determine the exact positions and qualitative behavior of these singularities. In addition to these geometrical singularities, we also find that the system shows order-disorder transitions, with a disordered phase at large lattice spacings, a phase with spontaneously broken orientational lattice symmetry at small lattice spacings, and an intervening Berezinskii-Kosterlitz-Thouless phase in between.

I. INTRODUCTION

In many molecular solids, the melting transition from the low-temperature crystalline solid phase to the high-temperature liquid phase does not occur in a single step, but one finds a multiplicity of mesophases. These are called "liquid crystals" or "plastic solids." In the former, the periodic three-dimensional crystal structure is absent, but a varying amount of orientational order may be present. In the latter, the average positions of the centers of masses of the molecules do lie on a three-dimensional crystalline lattice, but there is no or only partial orientational order. These were originally called plastic solids, as they can be easily deformed using much less force, compared to "hard" crystals. Some examples of common materials that show plastic solid phases are nitrogen [1], carbon tetrabromide [2], and formylferrocene [3]. The currently favored nomenclature for these is orientationally disordered crystals. In recent years, these have attracted a lot of interest because of their promising applications in diverse areas such as solid electrolytes [4], drug delivery [5], optoelectronics [6], barocalorics [7], piezoelectrics [8], etc. For a recent review of the applications, see Das *et al.* [9].

In 1930, Pauling derived a rough criteria for the strongly hindered rotational motion of molecules in crystalline solids [10]. But it was Timmermans who systematized the phenomenological study of plastic crystals starting from the 1930s [11]. On the theoretical front, Pople and Karasz [12] extended the two-lattice model of Lennard-Jones and Devonshire [13] to account for the order-disorder transition in the orientation of molecular crystals. A minimal model for these would be to assume the constituents as rigid objects, each identically pivoted on a lattice and free to rotate provided no objects overlap with each other. Casey and Runnels [14] and Freasiers and Runnels [15] examined a system of hard squares with centers fixed on the one-dimensional (1D) lattice. We have recently discussed this model and called it rigid hard rotors on a lattice as a model of multiple phases shown by plastic crystals to describe the transitions between them [16–18]. Note that since the lattice is always present, the model does not have a "liquid" phase with no crystalline order.

In an earlier paper [18], we determined the exact functional form of the one-point probability distribution function of orientations at a site for a range of lattice spacings when a particular condition, called the at-most one overlap (AOO) condition, holds. In this paper, we particularly examine a system of hard disks asymmetrically pivoted on a triangular lattice and study the one-point probability distribution function (PDF) $P(\theta)$ of orientations θ beyond the AOO condition. We find that the distribution function $P(\theta)$ shows cusp singularities. We determine the exact position and qualitative behavior beyond the AOO condition. Singularities in the pair distribution function have been studied earlier by Stillinger [19] and numerically observed in the probability distribution of bond-pair angles in a system of hard spheres [20], but here we discuss nontrivial singularities in the one-point function. We also numerically verify our findings with the help of Monte Carlo simulations.

This paper is organized as follows. In Sec. II, we define our model. In Sec. III, we show that there exist multiple cusp singularities in the one-point probability distribution of orientations and exactly determine their nature and positions. In Sec. IV, we verify our findings using Monte Carlo simulations. Section V contains some concluding remarks.

II. MODEL

We consider a system of identical unit-radius circular disks, each with an asymmetrically placed pivot at a distance

---

*Corresponding author: ss0410@princeton.edu
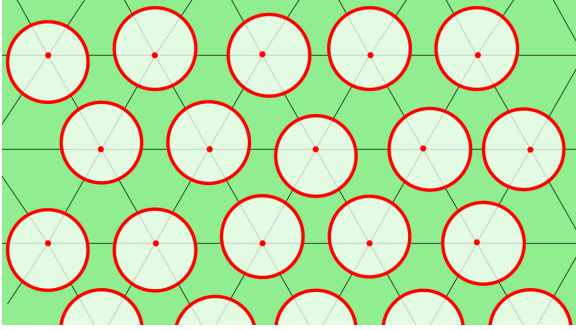†deepak@iiserpune.ac.in

FIG. 1. A set of unit-radius hard circular disks pivoted asymmetrically on the triangular lattice with lattice spacing a. The pivot is placed at a distance ϵ from the center.

ϵ from the center, as shown in Fig. 1. The pivots form a regular triangular lattice with lattice spacing a, and the disks can rotate freely about the pivots, with the constraint that no disks can overlap with each other. The orientation of a disk pivoted at lattice site $\mathbf{r}$ is specified by an angle $\theta(\mathbf{r})$, measured between the long axis (passing through the pivot and center) and the x axis. From elementary geometry, it is clear that if $a > 2(1 + \epsilon)$, the disks rotate freely and the closest-packing limit is reached when $a = 2$. We write lattice spacing a as

$$a = 2 + \epsilon x, \quad (1)$$

with $0 \leqslant x \leqslant 2$.

The partition function of the system having N disks is

$$\mathcal{Z}_N = \left[\prod_{\mathbf{r}} \int_{-\pi}^{\pi} \frac{d\theta(\mathbf{r})}{2\pi} \right] \prod_{\substack{\mathbf{x,y} \\ \mathbf{x} \neq \mathbf{y}}} \{1 - \eta[\theta(\mathbf{x}), \theta(\mathbf{y})]\}, \quad (2)$$

where $\eta[\theta(\mathbf{x}), \theta(\mathbf{y})]$ is an indicator function which is one when disks at sites $\mathbf{x}$ and $\mathbf{y}$ with orientations $\theta(\mathbf{x})$ and $\theta(\mathbf{y})$, respectively, overlap, and zero otherwise. We define the entropy per site $s(x, \epsilon)$ by

$$s(x, \epsilon) = \lim_{N \to \infty} \frac{\ln \mathcal{Z}_N}{N}. \quad (3)$$

As ϵ tends to zero, the function $s(x, \epsilon)$ has a well-defined nontrivial limit,

$$s(x) = \lim_{\epsilon \to 0} s(x, \epsilon). \quad (4)$$

In this limit, the no-overlap condition between two neighboring sites simplifies. For two neighboring rotors, if the line joining the pivots makes an angle ϕ with the x axis, the no-overlap condition to first order in ϵ becomes

$$x - \cos(\theta - \phi) + \cos(\theta' - \phi) \geqslant 0. \quad (5)$$

In Fig. 2, we compare the plots of $P(\theta)$ for $\epsilon \to 0$ and $\epsilon = 0.2$ using Monte Carlo simulations. We see that the qualitative behavior of $P(\theta)$ is the same for the two cases.

The limit $\epsilon \to 0$ has the advantage that the number of parameters specifying the model is reduced to 1. In the following, for the sake of simplicity, we restrict our discussion
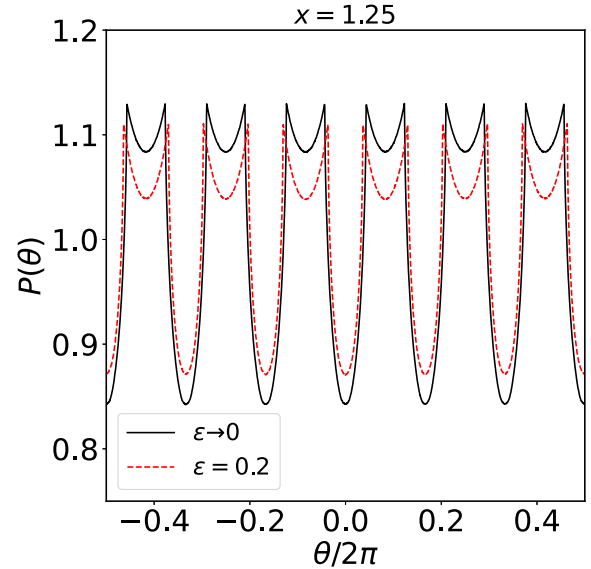

FIG. 2. Comparison of $P(\theta)$ for finite ϵ and $\epsilon \to 0$ at $x = 1.25$.

to this case. The case of more general ϵ presents no additional special features, as evident from Fig. 2.

This model can also be thought of as a system of planar spins $\{\theta(\mathbf{r})\}$ on the vertices of a triangular lattice, with nearest-neighbor interaction Hamiltonian $\mathcal{H}$ given by

$$\mathcal{H} = J \sum_{\mathbf{r}} \sum_{j=0}^{2} \Theta\{\cos[\theta(\mathbf{r}) - j\pi/3] - \cos[\theta'_j(\mathbf{r}) - j\pi/3] - x\}, \quad (6)$$

where $\theta'_j(\mathbf{r})$ is the neighboring spins of the spin $\theta(\mathbf{r})$ in the lattice direction $j\pi/3$, and $\Theta(x)$ is the Heaviside step function of x. The hard-core limit corresponds to setting J to $+\infty$.

This model is of the same form as the model of hard-core spins studied earlier by Sommers *et al.* [21]. These authors studied the case where our condition (5) is replaced by $|\theta - \theta'| \leqslant \alpha$. The qualitative behavior of the models is similar. The main difference where our model differs from theirs is the explicit breaking of isotropy in the spin space by the lattice-direction-dependent interaction. In particular, the cusp singularities that we discuss here are not present in the hard-core spin model.

III. PROBABILITY DISTRIBUTION OF ORIENTATIONS

Let $P(\theta)d\theta$ denote the probability that the disk that was pivoted to a randomly picked site in the equilibrium ensemble described by the partition function in Eq. (2) is at an orientation between θ and $\theta + d\theta$.

A. At-most one overlap (AOO)

The simplest case is when x lies in the range $[1 + \sqrt{3}/2, 2]$. In this case, it is easily seen that in any configuration of orientations of disks, any disk can overlap with, at most, one other disk. It was called the AOO condition in our earlier paper [18]. We showed that within the AOO regime, the partition function

simplifies to the calculation of the partition function of dimers and vacancies on the same lattice, where the activity of dimers is given by

$$z = -\int_{-\pi}^{\pi} \frac{d\theta}{2\pi} \int_{-\pi}^{\pi} \frac{d\theta'}{2\pi} \eta(\theta, \theta'). \quad (7)$$

We also obtained an explicit expression for $P(\theta)$, involving an undetermined function $\bar{n}(z)$, which gives the number density of dimers $\bar{n}(z)$ as a function of their activity z within the AOO regime in d dimensions. Following this general expression, the one-point PDF in the present scenario is given by

$$P(\theta) = [1 - 2\bar{n}(z)]\left[1 + \frac{\bar{n}(z)}{3z[1 - 2\bar{n}(z)]} \sum_{i=1}^{6} f_i(\theta)\right], \quad (8)$$

where $f_i(\theta)$ is given by

$$f_i(\theta) = \int_{-\pi}^{\pi} \frac{d\theta_i}{2\pi} \eta(\theta, \theta_i), \quad (9)$$

and $\bar{n}(z)$ is the dimer number density at activity z, which is given by the low-density expansion,

$$\bar{n}(z) = \sum_{n=1}^{\infty} (-1)^{n-1} a_n z^n, \quad (10)$$

where a_n is the number of heaps made of dimers [22]. For the triangular lattice, we have

$$\bar{n}(z) = 3[z - 11z + 144z^2 - 2047z^3 + 30526z^4 + \cdots]. \quad (11)$$

In our problem, the explicit expression for the function $\eta(\theta, \theta_1)$ is (see Fig. 3 for more details)

$$\eta(\theta, \theta_1) = \begin{cases} 1 & \text{if } |\theta| \leqslant \arccos(x - 1) \text{ and } |\theta_1| \geqslant \arccos[\cos(\theta) - x] \\ 0 & \text{otherwise.} \end{cases} \quad (12)$$

Then, it is easily seen that $f_1(\theta)$ is given by

$$f_1(\theta) = \begin{cases} 2\{\pi - \arccos[\cos(\theta) - x]\}, & |\theta| \leqslant \arccos(x - 1) \\ 0 & \text{otherwise.} \end{cases} \quad (13)$$
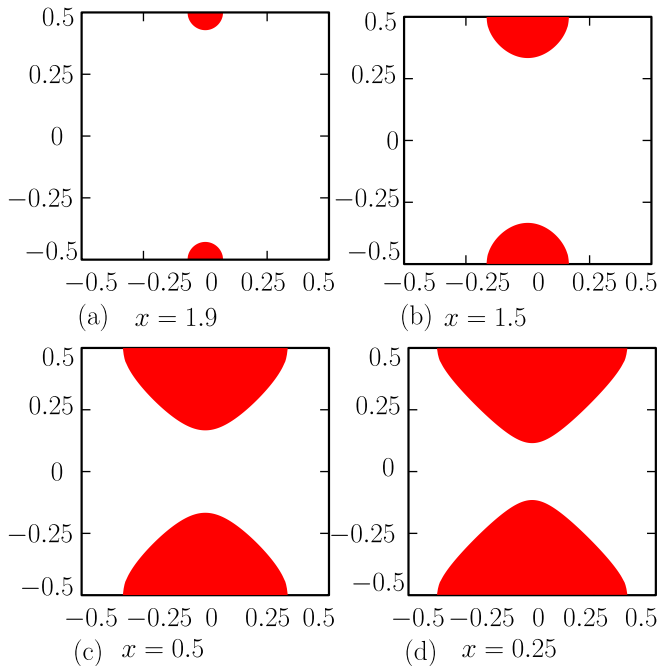
Other f_i's can be easily found using the symmetries of the underlying lattice. From this, it is easily seen that $P(\theta)$ has square-root cusp singularities (see the Appendix for more details) at

$$\theta_{\text{cusp}} = \frac{j\pi}{3} \pm \arccos(x - 1), \quad (14)$$

where $j = 0, 1, 2, \ldots, 5$.

B. Beyond the AOO condition

Now, we consider x outside the regime where the AOO condition holds. When $x = 1 + \sqrt{3}/2 - \delta$, with δ positive but small, the AOO condition is no longer satisfied. In this case, one can still define the graphical expansion of Eq. (2) in terms of configurations of dimers, but now the configurations where two or more dimers are incident on a vertex have nonzero weight. However, if δ is small, the weights of such vertices are small. This suggests that we can organize the terms of this series in the following form:

$$\mathcal{Z} = \mathcal{Z}_0 + \mathcal{Z}_1 + \mathcal{Z}_2 + \cdots. \quad (15)$$

In this expansion, $\mathcal{Z}_r$ is the sum over terms having r dimer pairs such that the dimers in each pair have a common vertex. We may associate an extra factor y with each such overlapping dimer pair, and consider the partition sum

$$\mathcal{Z}(y) = \sum_{r=0}^{\infty} y^r \mathcal{Z}_r. \quad (16)$$

We treat y as a small parameter and, assuming the sum converges for small enough y, treat it as a perturbation series in y.
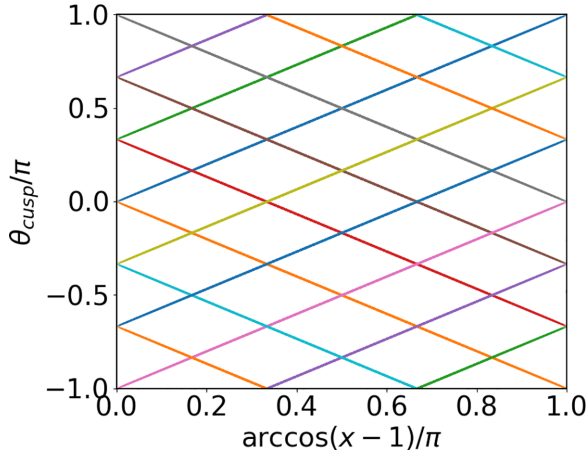

FIG. 3. $\eta(\theta, \theta')$ for nearest-neighbor disks along the x axis for different values of x when $\epsilon \to 0$ in the $(\frac{\theta}{2\pi}, \frac{\theta'}{2\pi})$ plane. The shaded area (red) corresponds to the overlap region where η is 1. In the unshaded area, $\eta = 0$. For other nearest-neighbor pairs, $\eta(\theta, \theta')$ can be similarly obtained using the symmetries of the triangular lattice.

FIG. 4. The change in the position of cusp singularities in $P(\theta)$ as we vary x. The positions vary linearly with the variable arccos $(x-1)$.

If we put $y = 0$ in this series, we have a sum over all the dimer configurations. In this ensemble, one can define the one-point function $P(\theta)$ as

$$P(\theta) = \sum_{\mathbf{x}} \langle \delta[\theta(\mathbf{x}) - \theta] \rangle, \tag{17}$$

where the angular brackets denote the average over the ensemble. It is easy to see that in the unperturbed ensemble $\mathcal{Z}_0$, Eq. (8) continues to remain valid, but now in this ensemble there are ranges of θ where more than one of the f terms contributes in the equation. And the positions of the cusp singularities in $P(\theta)$ are still given by Eq. (14).

Consider the terms in $\mathcal{Z}_1$, involving two specified dimers meeting at a specific site $\mathbf{x}$. Say the dimers are covering the bonds $(\mathbf{x}, \mathbf{y})$ and $(\mathbf{x}, \mathbf{z})$. This weight can be written as a product of two terms T_1 and T_2, with

$$T_1 = \int d\theta(\mathbf{x}) \int d\theta(\mathbf{y}) \int d\theta(\mathbf{z}) \; \eta(\mathbf{x}, \mathbf{y}) \eta(\mathbf{x}, \mathbf{z}). \tag{18}$$

It can be shown that for small positive δ, T_1 varies as [18] $\delta^{3/2}$. T_2 is a polynomial in z, the sum over all possible partial dimer coverings of the lattice, not involving sites $\mathbf{x}, \mathbf{y}, \mathbf{z}$. A similar statement is valid for higher r.

If we expand the function $P(\theta)$ in powers of y, each term in the perturbation sum is well behaved and only singularities in θ come from integration of the functions η, and hence the positions are the same as in Eq. (14) and are robust. By analytic continuation on y, we expect these results to hold for all y, and hence at $y = 1$. Thus, we conjecture that the cusp singularities $P(\theta)$ are given by Eq. (14) for all x, in the range $0 < x < 2$. This is shown in Fig. 4. Thus, the positions of the singularities do not change as long as we work within any finite order of the perturbation theory in y. Numerical evidence of this conjecture based on a Monte Carlo simulation is presented next.

IV. MONTE CARLO RESULTS

Now we present our findings of Monte Carlo simulations. Our simulations were done on lattices of size varying
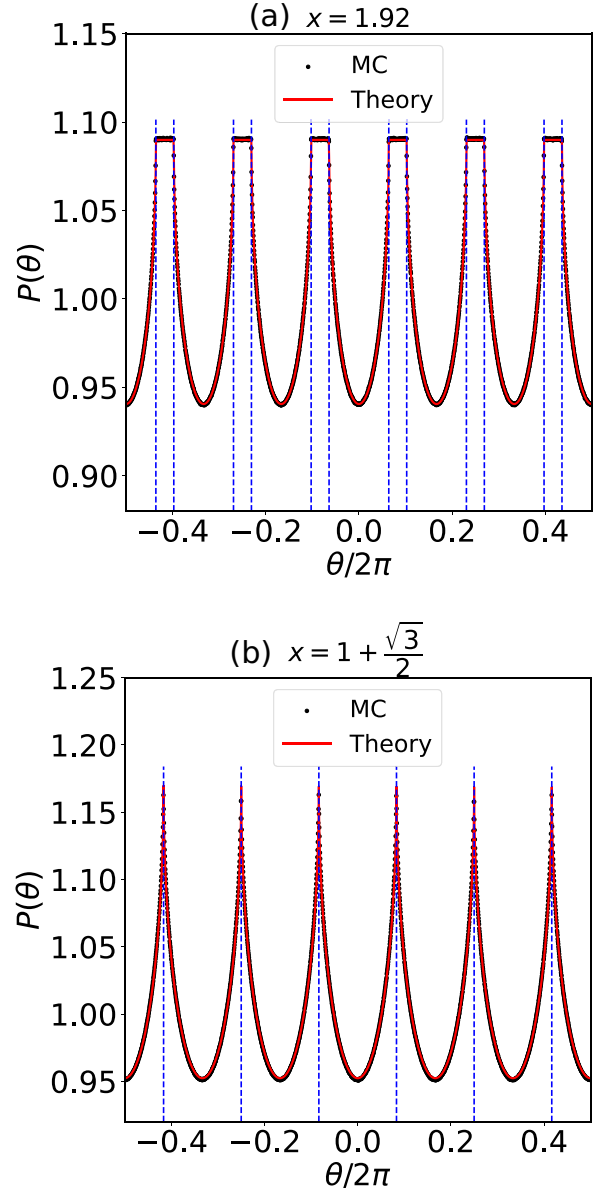

FIG. 5. One-point PDF under AOO regime. (a) $x = 1.92$ and (b) $x = 1 + \frac{\sqrt{3}}{2}$. Dashed vertical lines represent the positions of cusp singularities given in Eq. (14). Theoretical predictions, given by Eqs. (8) and (14), and Monte Carlo results are in very good agreement.

from 50×50 to 100×100. We use a single site update scheme: we pick a site $\mathbf{r}$ at random and try to change the value of $\theta_{\mathbf{r}}$ to $\theta_{\mathbf{r}} + \Delta\theta$, where $\Delta\theta$ is a random variable with a uniform distribution from $-\Delta_0$ to $+\Delta_0$. We accept the move if the new value does not result in any overlap. Then we repeat. We average over times of the order of 7.2 million MCS, after rejecting the first 8×10^5 steps.

In Fig. 5, a one-point PDF is plotted using Monte Carlo simulations along with our theoretical prediction (8) in the AOO regime, $1 + \sqrt{3}/2 \leqslant x \leqslant 2$. One can see that the Monte Carlo findings are in very good agreement with our theoretical prediction, given by Eq. (8). The dashed vertical lines correspond to the position of the cusp singularities in Eq. (14) and is
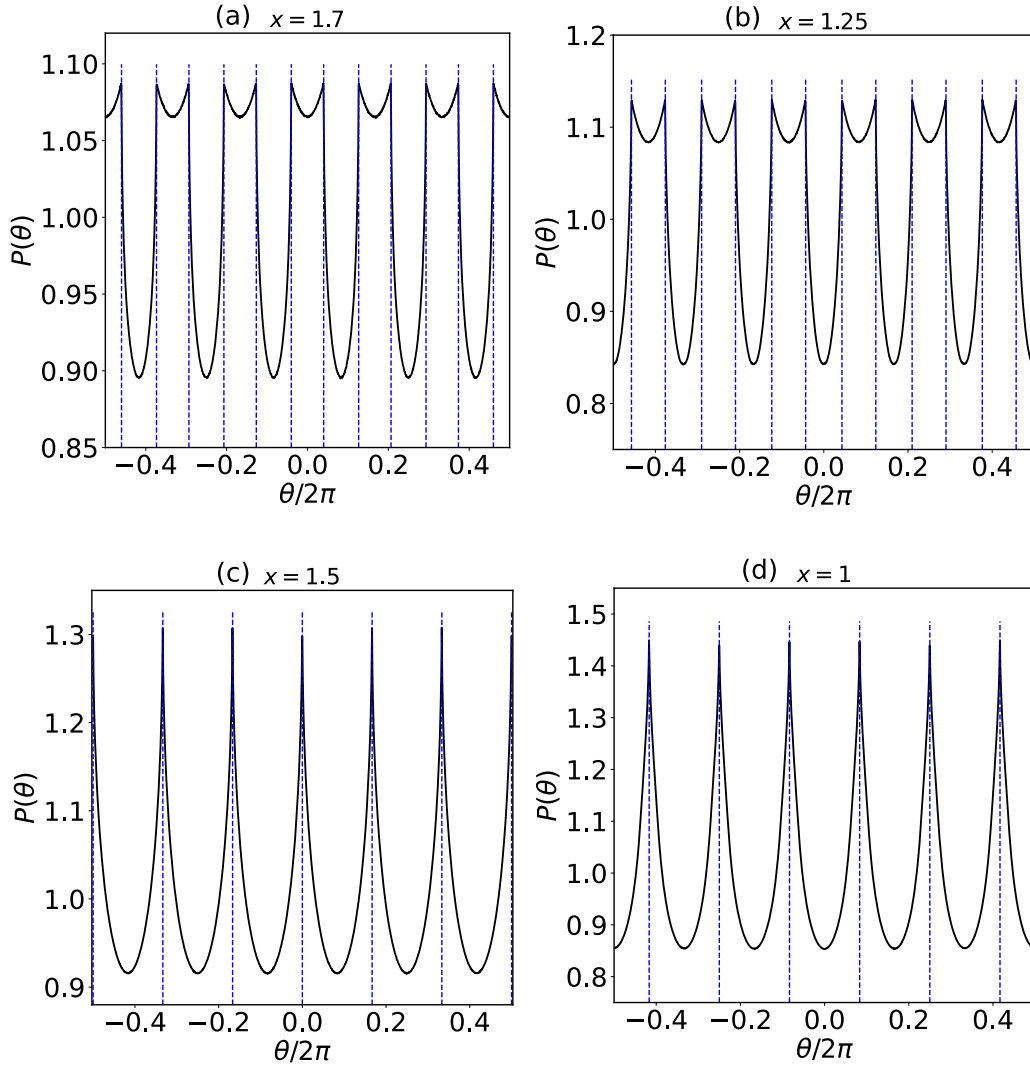
FIG. 6. One-point PDF beyond the AOO regime. (a) $x = 1.7$, (b) $x = 1.5$, (c) $x = 1.25$, and (d) $x = 1$. Dashed vertical lines represent the positions of the cusp singularities given in Eq. (14).

also in excellent agreement with the Monte Carlo simulations. Note that for $x = 1 + \sqrt{3}/2$, cusp singularities merge in pairs, producing only six singular points.

In general, there are 12 singularities for each value of x, except at special points where the singularities merge in pairs. We have determined the cusp positions from the Monte Carlo data for several values of x, shown in Fig. 6. These are in very good agreement with the predicted values.

We parametrize the distribution function for values of x outside the AOO regime using a fitting form with only one fitting parameter m, by

$$P_{\text{approx}}(\theta) = \mathcal{N} \prod_{i=0}^{5} [1 + m f(\theta - i\pi/3)], \quad (19)$$

where $\mathcal{N}$ is the normalization constant. Note that in the AOO regime, this expression is exact and the parameter m can be written in terms of the density of dimers. Outside the AOO regime, the expression is only approximate, but incorporates the known exact position of the cusp singularities, and its

analytical structure is suggested by the solution of the model of interacting rods on the Bethe lattice [17]. The plot shown in Fig. 7 compares the Monte Carlo data beyond the AOO regime, for $x = 1.7$ and 1.5, with value of m chosen to provide the best fit. We see that the ansatz provides a good qualitative description for the one-point PDF. The deviations from this form occur only in the intervals of θ for which the failure of the AOO condition is possible.

Our Monte Carlo simulations also revealed the presence of both the Berezinskii-Kosterlitz-Thouless (BKT) phase and the orientational-symmetry-broken phase in addition to the disordered phase. The clock model also exhibits a similar kind of behavior where there is an intervening BKT phase between the phases with broken symmetry and the disordered phase [23]. A phase where the symmetry of the orientational distribution function is broken under lattice rotations was observed for values of x less than 0.55, as illustrated in Fig. 8, where the one-point probability density function is peaked at $\pi/6$ and decays rapidly to zero as we move away from it. In the broken symmetry phase, all the singularities in $P(\theta)$ are seen
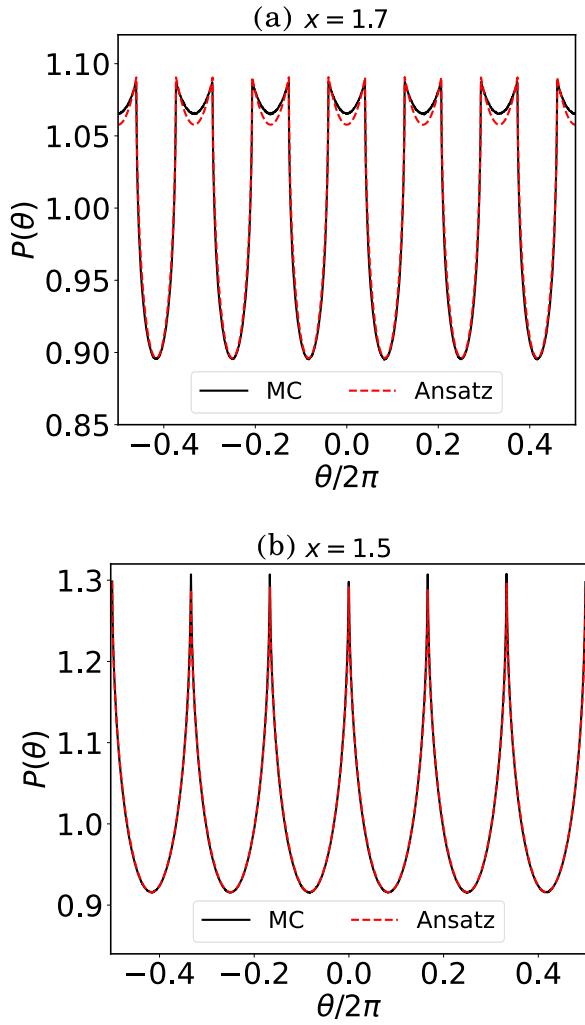
FIG. 7. Comparison of one-point PDF obtained using Monte Carlo simulations and our ansatz given in Eq. (19). (a) $x = 1.7$, $m = 1.405$ and (b) $x = 1.5$, $m = 1.32$.
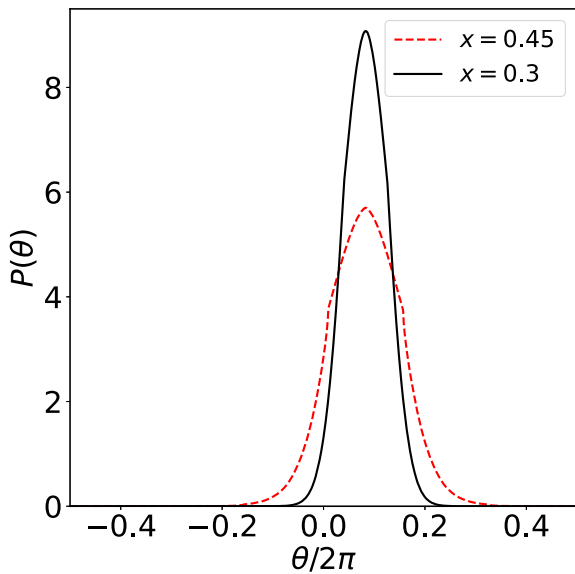

FIG. 8. One-point PDF obtained using Monte Carlo simulations for $x = 0.45$ (red dashed line) and $x = 0.3$ (black solid line).
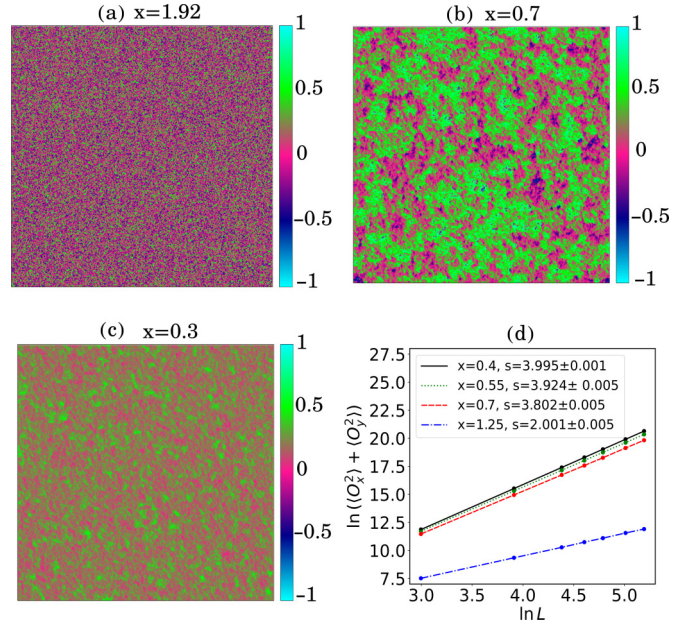

FIG. 9. (a)–(c) A spatial heat map of orientations of disks in a 600×600 triangular lattice for different x. Color coding is from -1 to 1 as orientations are divided by π. (a) At $x = 1.92$, the system is disordered, as one can see that all the orientations are randomly oriented, giving rise to no net ordering. (b) At $x = 0.7$, the system is critical as the cluster size of the same orientations exhibits large fluctuations. (c) At $x = 0.3$, the system is ordered as the orientations of the disks prefer to align along a direction giving rise to net ordering. (d) The ln‑ln plot of the mean square of the orientational order parameter vs L for different x. s represents the slope of the ln‑ln plots for various x.

only in the ensemble-averaged quantities, and not in the time averages of a single realization.

In the intermediate region, roughly in the range $0.55 < x < 0.9$, we observe the BKT phase which is usually characterized by a power-law decay of a correlation function with the exponent that depends on x and no long-range order. In Figs. 9(a)–9(c), spatial heat maps of the orientations of disks are plotted for different values of x chosen from three different phases.

The BKT phase can be identified by looking into the system size dependence of the mean square of the orientational order parameter. On an $L \times L$ lattice, the leading-order dependence of the mean square of the orientational order parameter on L for different phases varies as

$$\langle O_x^2 \rangle + \langle O_y^2 \rangle \propto \begin{cases} L^2 & \text{in the disordered phase} \\ L^4 & \text{in the ordered phase} \\ L^{4-\eta(x)} & \text{in the BKT phase,} \end{cases} \quad (20)$$

where $O_x = \sum_{\mathbf{r}} \cos \theta(\mathbf{r})$, $O_y = \sum_{\mathbf{r}} \sin \theta(\mathbf{r})$, and $0 \leqslant \eta(x) \leqslant 1/4$. The angular brackets represent the ensemble average. In Fig. 9(d), the mean square of the orientational order parameter vs L is plotted for various values of x. Our simulations show that for $x > 0.9$, we get a variance increasing as L^2, and for $x < 0.55$, it varies as L^4. It has an intermediate behavior, with $\eta \approx 0.08$, 0.15, and 0.20, for $x = 0.55$, 0.65, and 0.7, respectively. Nearer the BKT critical point, the relaxation

becomes slow and we are not able to get reliable estimates of the position of the critical point. In this paper, we do not try to identify the range of x values where the BKT phase occurs more precisely.

V. CONCLUDING REMARKS

The model discussed in this paper is of interest for several reasons. First, it is a model that is simple to define, which shows a large number of phases, and phase transitions, just by varying one parameter. It thus provides a minimal model for describing the multitude of phases seen in plastic solids.

Second, we have argued that to characterize the many phases, it is convenient to use not a single order parameter, but the whole distribution function of orientations. The full distribution as an order parameter has been discussed in the context of spin glasses [24]. Also, we have shown that this distribution function has robust geometrical singularities, whose qualitative behavior is easy to determine theoretically. Here we provide a system with continuous degrees of freedom that shows nontrivial singularities in the one-point function, whose position changes when the coupling constant is varied.

Third, we could determine the angular dependence of the distribution function $P(\theta)$ for a range of values on x, when the AOO condition is satisfied. Outside of this range, we showed that the distribution function can be expanded in a perturbation series in a variable y. In general, problems where the position of the singularity varies with the perturbation strength are difficult to construct. For example, the function $P(\theta)$ is expected to have cusp singularity of the form

$$P(\theta) = A(\theta, x) + B(\theta, x)|\theta - \theta_c(x)|^{1/2}, \quad (21)$$

near a cusp singularity $\theta = \theta_c(x)$, where $A(\theta, x)$ and $B(\theta, x)$ are smooth functions of x (different on different sides of the cusp). A naive perturbation series in $\delta = x - x^*$ for $P(\theta)$ about a point x^* would generate spurious singularities of the type $|(\theta - \theta_c(x^*)|^{-1/2}\delta$. Our perturbation parameter y avoids this problem, as the x-dependent cusp singularity structure is built in the perturbation series.

Fourth, the connection of this problem to the hard-disk problem is also of interest. Typical configurations generated in this model are visually not easily distinguished from the configurations of the hard-disk model at the same density. In the limit x tending to zero, we get the close-packed crystalline solid. In our model, the centers of the disks cannot move freely, but each center is restricted to a circle of radius ϵ. The restricted model seems to have qualitative behavior similar to the original model. For small x, we do not have crystalline order, and if we construct a local coarse-grained variable giving the average orientation of the lattice locally, this will change slowly in space, as in the hard-disk model. In particular, for $0 < x < 0.5$, one can show that there are no vortices possible.

For an intermediate range of x, we have seen that there is the Kosterlitz-Thouless phase, with power-law decay of the angular correlations.

In addition to these, the system shows a series of ordering transitions. In fact, for low x, our Monte Carlo simulations also show a transition to a glassy phase with very large correlation times. We have not discussed these here. This seems to be a good direction for further studies.

APPENDIX: SINGULARITIES IN $P(\theta)$

We will show that the $f_1(\theta)$ has square-root cusp singularities at $\theta_{\text{cusp}}^{\pm} = \pm \cos^{-1}(x - 1)$. If $\theta = \theta_{\text{cusp}}^{+} - \xi$ where $0 < \xi \ll 1$, then we have

$$\cos\theta - x = -1 + x\sqrt{2 - x}\,\xi + O(\xi^2). \quad (A1)$$

Let us define

$$y = \cos^{-1}[\cos\theta - x]. \quad (A2)$$

This can also be written as $\cos y = \cos\theta - x = -1 + x\sqrt{2 - x}\,\xi + O(\xi^2)$. If $\xi \to 0$, then $y \to \pi$. Therefore, we get

$$y = \pi - \sqrt{2x}\,(2 - x)^{1/4}\,\sqrt{\xi} + \text{higher-order terms in } \xi. \quad (A3)$$

Putting this in Eq. (13), we finally get

$$f_1(\theta) = \sqrt{2x}\,(2 - x)^{1/4}\sqrt{\theta_{\text{cusp}}^{+} - \theta} \quad \theta \to \theta_{\text{cusp}}^{+}. \quad (A4)$$

Following these same lines of argument, one can show that cusp singularity also exists at $\theta = \theta_{\text{cusp}}^{-} = -\cos^{-1}(x - 1)$. Other $f_i(\theta)$ can also be found from $f_1(\theta)$ using the symmetries of the triangular lattice, and thus $f_i(\theta) = f_1[\theta - (i - 1)\pi/3]$. Similarly, two cusp singularities exist for each $f_i(\theta)$, whose positions can be found using the symmetries of the triangular lattice. As a consequence, there exist 12 cusp singularities in $P(\theta)$, whose positions are given by

$$\theta_{\text{cusp}} = \frac{j\pi}{3} \pm \arccos(x - 1) \text{ where } j = 0, 1, 2, \dots, 5. \quad (A5)$$

[1] L. Tassini, F. Gorelli, and L. Ulivi, High temperature structures and orientational disorder in compressed solid nitrogen, J. Chem. Phys. **122**, 074701 (2005).

[2] B. M. Powell, V. F. Sears, G. Dolling, Neutron scattering from orientationally disordered solids, AIP Conf. Proc. **89**, 221 (1982).

[3] Y. Kaneko and M. Sorai, Heat capacity and phase transitions of the plastic crystal formylferrocene, Phase Trans. **80**, 517 (2007).

[4] J. M. Pringle, P. C. Howlett, D. R. MacFarlane, and M. Forsyth, Organic ionic plastic crystals: Recent advances, J. Mater. Chem. **20**, 2056 (2010).

[5] E. Shalaev, K. Wu, S. Shamblin, J. F. Krzyzaniak, and M. Descamps, Crystalline mesophases: Structure, mobility, and pharmaceutical properties, Adv. Drug Deliv. Rev. **100**, 194 (2016).

[6] Z. Sun, T. Chen, X. Liu, M. Hong, and J. Luo, Plastic transition to switch nonlinear optical properties showing the record high contrast in a single-component molecular crystal, J. Am. Chem. Soc. **137**, 15660 (2015).

[7] B. Li, Y. Kawakita, S. Ohira-Kawamura *et al.*, Colossal barocaloric effects in plastic crystals, Nature (London) **567**, 506 (2019).

[8] J. Harada, Y. Kawamura, Y. Takahashi, Y. Uemura, T. Hasegawa, H. Taniguchi and K. Maruyama, Plastic/ferroelectric crystals with easily switchable polarization: low-voltage operation, unprecedentedly high pyroelectric performance, and large piezoelectric effect in polycrystalline forms, J. Am. Chem. Soc. **141**, 9349 (2019).

[9] S. Das, A. Mondal, and C. L. Reddy, Harnessing molecular rotations in plastic crystals: A holistic view for crystal engineering of adaptive soft materials, Chem. Soc. Rev. **49**, 8878 (2020).

[10] L. Pauling, The rotational motion of molecules in crystals, Phys. Rev. **36**, 430 (1930).

[11] J. Timmermans, Plastic crystals: A historical review, J. Phys. Chem. Solids **18**, 1 (1961).

[12] J. A. Pople and F. E. Karasz, A Theory of fusion of molecular crystals: I. The effect of hindered rotation, J. Phys. Chem. Solids **18**, 28 (1961).

[13] J. E Lennard-Jones and A. F. Devonshire, Critical and co-operative phenomena IV. A theory of disorder in solids and liquids and the process of melting, Proc. R. Soc. London A **170**, 464 (1939).

[14] L. M. Casey and L. K. Runnels, Model for correlated molecular rotation, J. Chem. Phys. **51**, 5070 (1969).

[15] B. C. Freasier and L. K. Runnels, Classical rotators on a linear lattice, J. Chem. Phys. **58**, 2963 (1973).

[16] S. Saryal, J. U. Klamser, T. Sadhu, and D. Dhar, Multiple singularities of the equilibrium free energy in a one-dimensional model of soft rods, Phys. Rev. Lett. **121**, 240601 (2018).

[17] J. U. Klamser, T. Sadhu, and D. Dhar, Sequence of phase transitions in a model of interacting rods, Phys. Rev. E **106**, L052101 (2022).

[18] S. Saryal and D. Dhar, Exact results for interacting hard rigid rotors on a d-dimensional lattice, J. Stat. Mech. (2022) 043204.

[19] F. H. Stillinger, Pair distribution in the classical rigid disk and sphere systems, J. Comput. Phys. **7**, 367 (1971).

[20] A. Donev, S. Torquato, and F. H. Stillinger, Pair correlation function characteristics of nearly jammed disordered and ordered hard-sphere packings, Phys. Rev. E **71**, 011105 (2005).

[21] G. M. Sommers, B. Placke, R. Moessner, and S. L. Sondhi, From hard spheres to hard-core spins, Phys. Rev. B **103**, 104407 (2021).

[22] G. X. Viennot, Heaps of pieces, I : Basic definitions and combinatorial lemmas, in *Proceedings of the Colloque de Combinatoire Enumerative*, Lecture Notes in Mathematics Vol. 1234, edited by G. Labelle and P. Leroux (Springer, Berlin, Heidelberg, 1986), pp. 321–350.

[23] J. V. José, L. P. Kadanoff, S. Kirkpatrick, and D. R. Nelson, Renormalization, vortices, and symmetry-breaking perturbations in the two-dimensional planar mode, Phys. Rev. B **16**, 1217 (1977).

[24] M. Mezard, G. Parisi, and M. Virasoro, *Spin Glass Theory and Beyond* (World Scientific, Singapore, 1986).